Computer Simulation Studies of Equilibrium Properties in CS_2/C_6H_6 Liquid Mixtures

Silvia Dani[†] and Hubert Stassen*

Grupo de Química Teórica, Instituto de Química, Universidade Federal do Rio Grande do Sul, 91540-000 Porto Alegre-RS, Brazil

Received: May 13, 2003; In Final Form: September 26, 2003

Equilibrium properties for the binary liquid mixture CS_2/C_6H_6 at a temperature of 298 K and densities corresponding to liquid−vapor coexistence have been calculated by molecular dynamics computer simulation considering the molar fractions $x = 0.25$, $x = 0.5$, and $x = 0.75$ for the benzene compound. The intermolecular interactions are described by an all-atom model in a (12/6) Lennard-Jones format with electrostatic interactions represented by point quadrupoles localized on the molecular centers of mass. We have computed thermodynamic data and structural information in terms of radial and angular distribution functions. Obtained results are in accordance with experimental findings. The analysis of local molar fractions, as well as the internal energies of the mixtures, indicate that the liquid system CS_2/C_6H_6 presents many features of an ideal binary mixture. From the radial and angular correlations between CS_2 and C_6H_6 molecules, we conclude that first contact pairs prefer parallel configurations although no preferential ordering has been found within the first solvation shell.

1. Introduction

In the past decades, several studies have been dedicated to interactions between carbon disulfide and aromatic rings. From different types of experiments, it is suggested that the occurrence of gelation of atactic polystyrene in carbon disulfide might be due to a polymer−solvent complex with a structure that resembles a ladder with CS_2 molecules as the rungs.[1,2] The size of these cross-link domains favors the observed elastomeric gel formation.[2] Complexes involving CS_2 sulfur or similar sulfur atoms and phenyl rings are also observed in proteins.[3]

The system CS_2/C_6H_6 can be considered to represent a prototypical model for these kind of interactions. The binary liquid mixture has been studied by various dynamical spectroscopic techniques permitting the elucidation of interaction-induced effects. From excess absorption in the far-infrared absorption spectra of the mixture, the presence of transient clusters with lifetimes on the order of 0.1 ps has been suggested.[4] The cluster formation has been primarily attributed to packing effects and, secondarily, to quadrupolar electrostatic interactions.[5] In addition, depolarized light scattering spectra have been used to determine the orientations between CS_2 and C_6H_6 molecules by means of the orientational structure factor calculated from the purely orientational part of the spectrum. The obtained results exhibit the tendency to perpendicular orientations between CS_2 and C_6H_6 molecules in the liquid mixtures.[6] From the theoretical point of view, high-level ab initio calculations of the benzene−carbon disulfide 1:1 complex revealed a T-shaped and a parallel configuration between CS_2 and C_6H_6 as energetically favored.[7] Earlier theoretical studies of 1:1 complexes between aromatic molecules (C_6H_6, C_6F_6) and linear triatomics (CO_2, CS_2) illustrated the important role of quadrupolar interactions in defining the most stable configurations.[8]

In this article, we present thermodynamic and structural data for the binary mixtures of CS_2 with benzene focusing particularly on the relative orientations of the two compounds in the liquid state. Therefore, we have undertaken molecular dynamics (MD) computer simulations utilizing potential models for the compounds that have been established for the pure liquid phases of CS_2 and benzene. More details about the potential models are given in section 2 of the article. Computational details for the MD simulations are summarized in section 3. Our principal purpose is to elucidate local structures in the surroundings of the CS_2 and benzene molecules in the binary mixture. Thus, we have computed intermolecular atom−atom pair distribution functions, as well as radial distribution functions for center of mass distances as a function of the angle between the principal molecular axis (the molecular axis of the CS_2 molecules and the C_6 axis of the benzene molecules). The results of this analysis are discussed and compared with both experimental and theoretical findings in section 4, before finishing the present article with some conclusions in section 5.

2. Interaction Model

A realistic intermolecular potential model for describing liquid-state interactions has to fulfill several requirements. In addition to computational efficiency, the interaction model should predict the correct experimental properties concerning thermodynamics, phase equilibria, liquid structure, and dynamics. Even for fluids composed of almost spherical molecules, many of the published potential models do not coincide with all of these requirements.[9] Thus, to establish an interaction model for the binary mixture of CS_2 with benzene, we have carried out a careful analysis of already published interaction models for pure liquid CS_2 and benzene.

In the case of liquid CS_2, Tildesley and Madden (TM) constructed a three center (12/6) Lennard-Jones (LJ) potential[10] that has been successfully applied to simulate light scattering spectra,[11] far-infrared absorption,[12] and the shear viscosity coefficient[13] of pure CS_2, as well as several equilibrium,[14]

* Corresponding author. E-mail: gullit@iq.ufrgs.br.
[†] Also Departamento de Química, Universidade Luterana do Brasil, Rua Miguel Tostes 101, 92420-280 Canoas-RS, Brazil.

10.1021/jp0353136 CCC: $25.00
Published on Web 11/22/2003

TABLE 1: Liquid CS_2 Internal Energy, U (kJ/mol), Mean-Square Forces, F^2 (10^{-19} N^2), and Torques, N^2 (10^{-39} J^2), Integrated Correlation Times (ps) for the Linear (τ_v) and Angular Velocity (τ_w) TCFs, and Exponential Orientational Times (ps) for the First- (τ_1) and Second-Order (τ_2) Orientational TCFs

potential[a]	U	F^2	N^2	τ_v	τ_w	τ_1	τ_2
TM	−25.1	1.8	2.7	0.13	0.08	4.2	1.65
TMQ	−24.8	1.8	2.8	0.11	0.08	4.1	1.55

[a] TM represents the potential from ref 10. The TMQ potential includes molecular quadrupole point tensors at the carbon atoms in addition.

dynamical,[15] and spectroscopic features[16] in binary mixtures of CS_2 and CCl_4. Because of this broad variety of experiences, we have adopted the potential of TM for CS_2. To incorporate electrostatic interactions, we have added molecular quadrupole moments as point tensors located at the center of mass of the CS_2. In the following, we call this potential model the TMQ potential. As the molecular gas-phase quadrupole moment, we used 9.3×10^{-40} C m^2.[17] As becomes evident from Table 1, in which we compare several thermodynamic data and correlation times for simple time correlation functions (TCFs) between the TM and TMQ potential, the addition of point quadrupoles maintains the TM equilibrium and dynamical properties of liquid CS_2, at least at a temperature of 298 K and a density corresponding to liquid−vapor coexistence.

On the other hand, for the liquid state of C_6H_6, none of the numerous published potential models possesses the broad applicability of the TM potential. Several six-center potentials[18] furnish thermodynamic properties for liquid benzene in good agreement with experiment. However, 12-center interaction models are more suitable to discuss the structure of liquid benzene.[19] With respect to structural properties, liquid benzene modeled by the old 12-center Buckingham potential of Williams[20] compares well with experimental X-ray and neutron diffraction data,[21] but the functional form of the potential is not suited to combine with the CS_2 TM LJ potential. Thus, we have investigated the 12-center LJ potentials of Linse[22] with parameters established from quantum mechanical calculations on the benzene dimer[23] and the optimized potential for liquid simulations (OPLS)-based potential from Jorgensen and Severance[24] describing the electrostatic interactions in both models by point quadrupole moments localized as point tensors at the molecular centers of mass. Without any parameter manipulations, the Linse potential produces a liquid state corresponding to 298 K and liquid−vapor coexistence that is too strongly bound by approximately 4 kJ/mol. Thus, the LJ part of the Jorgensen potential combined with quadrupolar interactions has been selected to represent benzene in the mixtures.

In summary, considering molecules i and j with a center of mass separation r_{ij}, the van der Waals interaction energy of the pair is expressed as the sum of all of the atom−atom (12/6) LJ potentials between the n_i and n_j atoms of molecules i and j, respectively,

$$u_{ij}^{\mathrm{vdw}}(r_{ij},\Omega_i,\Omega_j) = \sum_{\alpha}^{n_i}\sum_{\beta}^{n_j} 4\epsilon_{\alpha\beta}\left[\left(\frac{\sigma_{\alpha\beta}}{r_{\alpha\beta}}\right)^{12} - \left(\frac{\sigma_{\alpha\beta}}{r_{\alpha\beta}}\right)^{6}\right] \qquad (1)$$

In eq 1, molecular orientations Ω_i are included by considering explicitly site−site distances $r_{\alpha\beta}$. The LJ parameters $\sigma_{\alpha\beta}$ and $\epsilon_{\alpha\beta}$ between different atoms are obtained by the Lorentz−Berthelot mixing rules,[25]

$$\epsilon_{\alpha\beta} = (\epsilon_{\alpha\alpha}\epsilon_{\beta\beta})^{1/2} \qquad \sigma_{\alpha\beta} = (\sigma_{\alpha\alpha} + \sigma_{\beta\beta})/2 \qquad (2)$$

with $\epsilon_{\alpha\alpha}$ and $\sigma_{\alpha\alpha}$ representing the potential well depth parameter for the interaction between two atoms of type α with effective diameter $\sigma_{\alpha\alpha}$. All of the LJ parameters and bond lengths used in this study are presented in Table 2.

The electrostatic interactions were evaluated from a multipole expansion. For molecules belonging to the $D_{\infty h}$ (CS_2) and D_{6h} (benzene) point groups, the first nonvanishing electrostatic multipole moment is the quadrupole Q. Neglecting contributions from higher multipole moments, the quadrupole−quadrupole interaction,

$$u_{ij}^{\mathrm{el}}(r_{ij},\Omega_i,\Omega_j) = \frac{1}{9}\mathbf{Q}_i{:}\mathbf{T}_{ij}^{(4)}{:}\mathbf{Q}_j \qquad (3)$$

represents our electrostatic pair potential. $\mathbf{T}_{ij}^{(4)}$ is the tensor of rank 4 obtained by 4-fold derivation of r_{ij}^{-1} with respect to the components of the center of mass separation vector $\mathbf{r}_{ij}$. Thus, an element of $\mathbf{T}^{(4)}(r_{ij})$ is defined by

$$T_{ij}^{\alpha\beta\gamma\delta}(r_{ij}) = \frac{\partial}{\partial r_{ij}^{\alpha}}\frac{\partial}{\partial r_{ij}^{\beta}}\frac{\partial}{\partial r_{ij}^{\gamma}}\frac{\partial}{\partial r_{ij}^{\delta}}\frac{1}{r_{ij}} \qquad (4)$$

with the Greek subscripts denoting Cartesian components. The quadrupole tensors $\mathbf{Q}_i$ depend on molecular orientation. For axial-symmetric charge distributions, the unit vector $\hat{\mathbf{u}}_i$ oriented along the molecule's principal axis (the molecular axis for CS_2 and the C_6 axis for benzene) determines the Cartesian tensor components of $\mathbf{Q}_i$ in the laboratory frame[26]

$$Q_i^{\alpha\beta} = \frac{3}{2}Q_0\left(\hat{u}_i^{\alpha}\,\hat{u}_i^{\beta} - \frac{\delta_{\alpha\beta}}{3}\right) \qquad (5)$$

Q_0 is the gas-phase value for the molecular quadrupole moment. In this study, we used the experimental value $Q_0 = 9.3 \times 10^{-40}$ C m^2 [17] for CS_2. For the benzene molecule, we have adopted the numerical value of $Q_0 = -24 \times 10^{-40}$ C m^2 that corresponds to the point charge model of the original benzene potential model.[24] The experimental quadrupole moment for the benzene molecule is $Q_0 = -30 \times 10^{-40}$ C m^2.[26]

3. Computational Details

The MD simulations were carried out for the pure liquids benzene and CS_2, as well as for mixtures of CS_2 with benzene at three molar fractions of benzene, $x = 0.25$, 0.50, and 0.75. All of the calculations are performed in the microcanonical ensemble (*NVE*) with 256 molecules (pure liquids) or 500 molecules (mixtures) arranged in a cubic box with dimensions corresponding to experimental densities for liquid−vapor coexistence at a temperature of $T = 298$ K. Periodic boundary conditions and a spherical cutoff (half of the box length) with the usual minimum image convention were applied to all of the distance-dependent properties.

Initial configurations were created arranging the molecules on fcc lattice positions with random orientations. In the case of mixtures, each fcc lattice point was randomly occupied by a molecule corresponding to one of the two compounds. Initial linear and angular velocities were chosen from the Maxwell−Boltzmann profiles corresponding to the desired temperature. During the simulations, the molecules were treated as rigid bodies describing the orientations via quaternions. The equations of motion for both translational and rotational motion were integrated using the fourth-order Gear−Nordsieck predictor−corrector algorithm[25] with an integration time step of $dt = 0.75 \times 10^{-15}$ s. Equilibration was achieved after approximately 25,

TABLE 2: LJ Parameters for CS_2 (Compound A) and Benzene (Compound B) and the Cross Interactions and the Bond Lengths, *d*

	CS_2-CS_2[10]			$C_6H_6-C_6H_6$[24]			$CS_2-C_6H_6$			
	C_A-C_A	S−S	C_A-S	C_B-C_B	H−H	C_B-H	C_A-C_B	C_A-H	$S-C_B$	S−H
ϵ/k (K)	51.2	179.0	95.7	35.2	15.1	23.1	42.5	27.8	79.4	52.0
σ (Å)	3.35	3.52	3.44	3.55	2.42	2.93	3.45	2.89	3.54	2.97
d (Å)			1.57	1.395		1.08				

TABLE 3: Simulation Parameters[a]

x_B[b]	number of molecules	molar volume[c] (cm^3/mol)	total time of simulation (ps)	cutoff (Å)
0	256	60.57	100	14.75
0.25	500	68.72	120	19.25
0.50	500	76.06	120	19.91
0.75	500	83.46	120	20.54
1	256	88.87	115	16.78

[a] The temperature is 298 K for all of the simulations. [b] x_B is the molar fraction for the benzene compound. [c] The molar volumes were computed from densities given in ref 4.

TABLE 4: Internal Energies, *U*, Total Energies, *E*, and Heats of Vaporization, ΔH_{vap}, for the Simulated Molar Fractions, x_B, of the Benzene Compound and Experimental Heats of Vaporization, ΔH_{vap}^{exptl} [a]

x_B	U	E	ΔH_{vap}	ΔH_{vap}^{exptl}	U_{vdw}	U_{el}
0	−24.8	−18.6	27.3	27.5	−24.6	−0.2
0.25	−26.3	−19.7	28.8	28.7	−25.5	−0.8
0.50	−28.0	−21.0	30.4	30.1	−26.6	−1.4
0.75	−29.6	−22.5	32.1	31.9	−27.4	−2.2
1	−32.2	−24.9	34.7	33.8	−29.2	−3.0

[a] All energies and enthalpies are in kJ/mol.

40, and 45 ps for pure CS_2, C_6H_6, and the mixtures, respectively. The simulation parameters are depicted in Table 3.

The simulation runs have been controlled by constancy in the total energy. Due to the small integration time step, the trajectories for all of the simulations were very stable exhibiting drifts in the total energy of less than 10^{-3} kJ/mol in 10 000 time steps.

Results and Discussion

4.1. Thermodynamic Data. In Table 4, we present some of the thermodynamic data of our simulations. Internal energies, U, have been converted into heats of vaporization, ΔH_{vap}, by

$$\Delta H_{vap} = -U + RT \tag{6}$$

where the usual approximations (vapor phase is ideal, neglecting volume changes in the liquid phase) are assumed to be valid. Experimental ΔH_{vap} for the mixtures have been calculated from data for the pure liquids taking into account excess enthalpies of mixing H_{mix}^{E}.[27] Comparing with the experimental heats of vaporization, we find a very good agreement between the simulations and experiment as illustrated in Table 4.

Also included in Table 4 are the internal energies stemming from van der Waals, U_{vdw}, and electrostatic, U_{el}, pair interactions as defined by eqs 1 and 3, respectively. These data indicate that electrostatic interactions from quadrupole tensors at the centers of mass produce approximately 10% of the internal energy in liquid benzene but are negligible in liquid CS_2. Increasing the molar fraction of benzene in the mixtures comes along with an almost linear increase in the electrostatic contribution to the internal energy. The main reason for this behavior is the large value for the gas-phase quadrupole moment of the benzene molecule (see section 2).

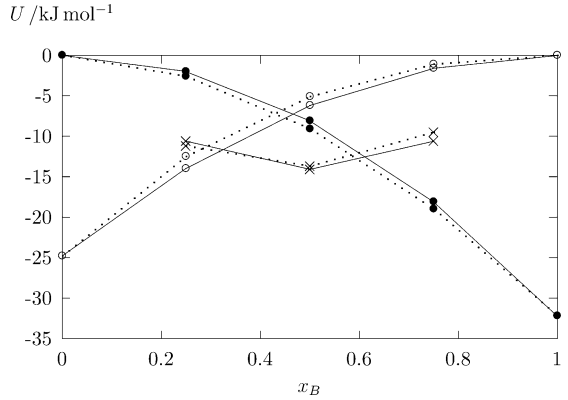

Figure 1. Partial internal energies, U_{AA} (○), U_{AB} (×), and U_{BB} (●) from the simulations (connected by the dotted line) and for an ideal mixture (connected by the full line) as defined by eq 7. x_B is the benzene molar fraction (A = CS_2, B = benzene).

A rough estimate for ideality in the CS_2/C_6H_6 mixtures has been obtained from the computed partial internal energies, U_{AA}, U_{AB}, and U_{BB} (A = CS_2, B = benzene) as a function of the molar fractions x_A and x_B. In Figure 1, these partial internal energies from the simulations are compared with ideal values evaluated by

$$U_{AA}^{id} = x_A^2 U_A$$
$$U_{AB}^{id} = 2x_A x_B \sqrt{U_A U_B}$$
$$U_{BB}^{id} = x_B^2 U_B \tag{7}$$

U_A and U_B representing the internal energies from the pure liquids. As Figure 1 indicates, CS_2-CS_2 interactions in the mixtures are weaker than suggested by the ideal model described by eq 7, whereas benzene−benzene interactions produce a weak excess toward more negative internal energies. As a consequence of this partial cancellation in the excess internal energy, the total energy U from Table 4 characterizes an almost ideal mixture.

4.2. Center of Mass Pair Distribution Functions. Quite generally, radial distribution functions furnish structural information about a liquid. Although the structure of molecular liquids has to be evaluated from pair distribution functions reflecting the relative molecular orientations, the center-of-mass (COM) pair distribution function, $g(r)$, represents an important property permitting the analysis of the local environment, especially in liquid mixtures. In Figures 2−4, the COM−COM pair distribution functions for CS_2-CS_2, benzene−benzene, and CS_2−benzene pairs of our simulations are illustrated.

The $g(r)$ for the CS_2 pairs in Figure 2 shows that the shape of the first peak in the $g(r)$ is not affected by the benzene molecules. Independent of the benzene concentration, the first solvation shell for CS_2 molecules surrounding CS_2 maintains a maximum position at 4.5 Å. The peak height of this function increases slightly and monotonically with the benzene concen-

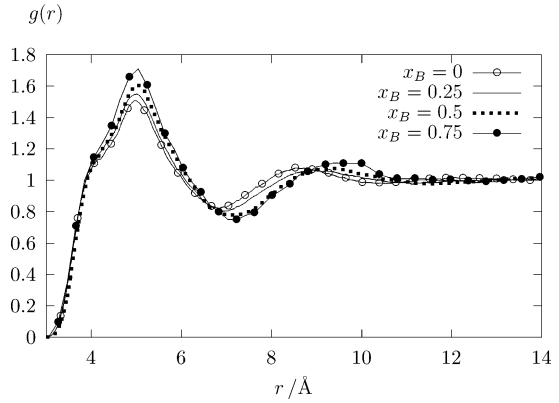

Figure 2. Intermolecular center of mass pair distribution function $g(r)$ for the CS_2 molecules as a function of the molar fraction x_B for the benzene component.

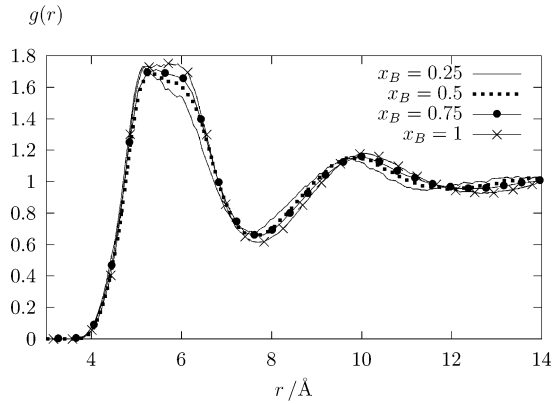

Figure 3. Intermolecular center of mass pair distribution function $g(r)$ for the benzene molecules as a function of the molar fraction x_B for the benzene component.

tration. The short distance branch of the CS_2-CS_2 pair distribution up to a shoulder at 3.9 Å is not affected by the addition of benzene indicating that nearest-neighbor configurations between CS_2 molecules remain as those in the pure liquid. Beyond the first peak, the addition of benzene molecules to CS_2 shifts the first minimum and second maximum toward longer distances.

The benzene−benzene pair distribution function from Figure 3 exhibits similar features. Adding CS_2 to benzene does not affect the short distance distribution of benzene pairs up to 5 Å. However, the shape of the first peak in the benzene−benzene distribution is somehow influenced beyond the peak maximum by the CS_2 addition. The broad peak observed in pure benzene is slightly straightened by adding CS_2. The formation of a shoulder at 6 Å is observed in the mixture with the highest CS_2 concentration. Positions of additional minima and maxima in the benzene−benzene $g(r)$ shift toward smaller distances when CS_2 is added.

The distribution of benzene−CS_2 pairs is depicted in Figure 4. As observed in the CS_2-CS_2 and benzene−benzene distribution functions, the first peak keeps the maximum position at 5.1 Å and changes only slightly the peak height when the benzene concentration increases. Beyond the first peak maximum, adding benzene causes a shift of additional extrema in the $g(r)$ toward larger distances.

The weak concentration dependence of the COM−COM pair distributions resembles the behavior that one might expect for an almost ideal mixture. The observed trend that the $g(r)$ shift slightly to larger distances when benzene is added to the

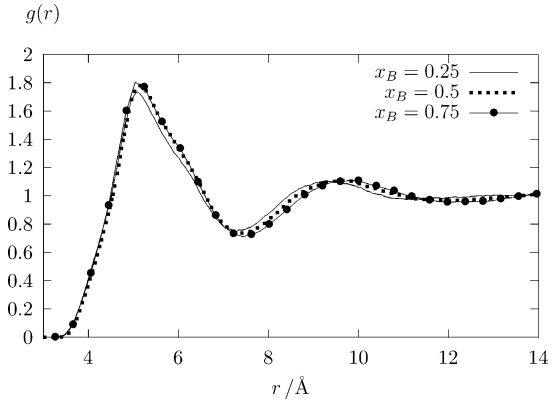

Figure 4. Intermolecular center of mass pair distribution function $g(r)$ for CS_2−benzene pairs as a function of the molar fraction x_B for the benzene component.

mixtures reflects the molar volume of the pure liquids and might be related to the larger molecular shape of the benzene molecules.

As another indicator for the ideality of a liquid mixture, we studied local mole fractions X_{IJ} of the *I*th component surrounding a molecule of component *J*. Using the corresponding partial coordination number $n_{IJ}(r)$, one defines the local mole fraction by

$$X_{IJ} = \frac{n_{IJ}(r)}{n_J(r)} \tag{8}$$

where $n_J(r)$ represents the total coordination number of a molecule belonging to component *J* of the mixture. The coordination numbers $n_{IJ}(r)$ are obtained by integrating the corresponding COM−COM pair distribution function $g_{IJ}(r)$,

$$n_{IJ}(r') = 4\pi\rho_I \int_0^{r'} r^2 g_{IJ}(r)\, \mathrm{d}r \tag{9}$$

In eq 9, ρ_I is the macroscopic number density of component *I*. The integration is usually restricted by the position of the first minimum in the pair distribution function permitting the determination of inhomogeneities within the first solvation shell around a chosen molecule of component *J*. This analysis has previously been applied to binary mixtures of CS_2 in CCl_4[14] and methanol in chloroform,[28] as well as aqueous solutions of DMSO[29] and formamide.[30]

Another parameter related to X_{IJ} is given by the sum of local mole fractions,

$$X_S = X_{II} + X_{JJ} \tag{10}$$

In homogeneous mixtures, the local molar fractions X_{II} and X_{JJ} are equal to the global mole fractions. Tendencies of demixing are indicated by $X_S > 1$, whereas $X_S < 1$ has been interpreted as association or cluster formation.[31] Numerical values for the first shell coordination numbers n_{IJ} and molar fractions X_{IJ} are summarized in Table 5. To define consistent solvation shells for a molecule of the *J* component, we have performed the numerical integration (eq 9) over the pair distribution functions for the mixtures up to the position of the first minimum in the $g(r)$ for the pure liquid of component *J*.

The local coordination numbers and molar fractions from Table 5 confirm our conclusions drawn from the partial internal energies in the preceding subsection. All of the studied compositions of the CS_2/benzene mixture exhibit local mole fractions in perfect agreement with the global composition. The

TABLE 5: Partial Coordination Numbers, n_{IJ}, and Local Mole Fractions, X_{IJ}, of the CS_2/Benzene Mixtures[a]

	x_B[b]				
	0	0.25	0.5	0.75	1
n_{BB}		3.04	6.01	8.75	12.55
n_{AB}		8.94	5.91	2.84	
n_{BA}		2.98	5.91	8.51	
n_{AA}	12.77	8.79	5.75	2.83	
n_B		11.98	11.92	11.59	12.55
n_A	12.77	11.77	11.66	11.34	
X_{BB}		0.25	0.50	0.75	1
X_{AB}		0.75	0.50	0.25	
X_{BA}		0.25	0.50	0.75	
X_{AA}	1	0.75	0.50	0.25	
X_S	1	1	1	1	1

[a] The subscripts A and B represent CS_2 and benzene component, respectively. [b] x_B is the mole fraction of benzene.

COM−COM pair distributions studied here correspond to homogeneous (ideal) mixtures. Thus, small shifts in the $g(r)$ from Figures 2−4 due to changes in the composition of the mixtures are a consequence of the density.

4.3. Angular Correlations. The atom−atom pair distribution functions, $g_{\alpha\beta}(r)$, permit a more detailed analysis of the liquid structure, especially within the first shell of coordination. In the case of the CS_2 molecules, the structural features of CS_2 pairs are revealed by the three atom−atom pair distributions, $g_{CC}(r)$, $g_{CS}(r)$, and $g_{SS}(r)$. A detailed discussion of these functions is given in refs 10 and 32. In summary, CS_2 pairs present preferentially parallel configurations at very short distances but are more perpendicularly oriented at distances corresponding to the first shell maximum. The atom−atom pair distribution functions $g_{CC}(r)$, $g_{CH}(r)$, and $g_{HH}(r)$ for benzene pairs are also well-known.[24,33] These functions are affected by more perpendicular orientations within the first shell but exhibit parallel orientations for closest-contact pairs as a result of packing effects.[34,35]

We computed all of the atom−atom pair distribution functions between CS_2 pairs and benzene pairs in the mixtures. However, the comparison of these functions for the mixtures with the data set for the pure liquids shows that the atom−atom pair distributions for CS_2 pairs and benzene pairs in the mixtures undergo only very small changes in peak positions and amplitudes. Thus, one might conclude that the structural characteristics of CS_2 pairs and of benzene pairs are not affected by any changes in the molar fractions of the components. For this reason, we do not present the six atom−atom pair distributions mentioned above.

To extract some structural information concerning CS_2−benzene pairs, we have computed their atom−atom pair distribution functions, $g_{CC}(r)$, $g_{CS}(r)$, $g_{HC}(r)$, and $g_{HS}(r)$ (discussed below), as well as the angle θ between the C_6-axis of the benzene molecules and the molecular axis of the CS_2 particles. The averaged cosine $\langle\cos\theta(r)\rangle$ for this angle as a function of the COM−COM distance r is defined by

$$\langle\cos\theta(r)\rangle = \frac{1}{N}\left\langle\sum_{i=1}^{N}\sum_{j\neq i}^{N}\delta(r - r_{ij})|\cos\theta_{ij}|\right\rangle \qquad (11)$$

where the average on the right-hand side (rhs) indicates sampling along the trajectory. For D_{6h} and $D_{\infty h}$ molecular species, pair configurations with angles θ and $\pi - \theta$ cannot be distinguished from each other. Thus, we have included in eq 11 only the absolute value for cos θ.

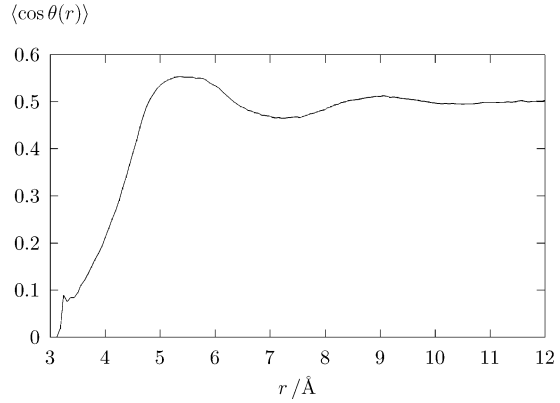

Figure 5. Average cosine $\langle\cos\theta(r)\rangle$ for the angle between the C_6-axis of the benzene molecules and the molecular axis of the CS_2 molecules as a function of the COM−COM distances in the equimolar mixture.

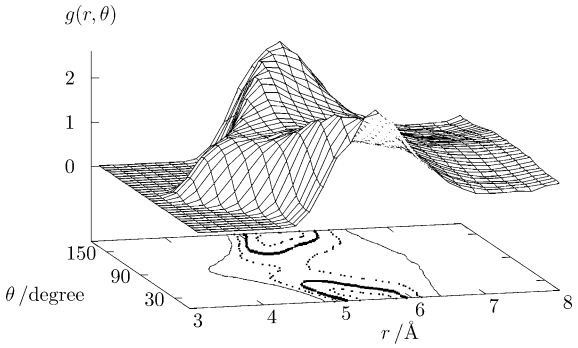

Figure 6. $g(r,\theta)$ as defined by eq 12 for the equimolar mixture. To facilitate the identification of characteristic angles and distances, some of the contour lines are shown in the r,θ-plane.

For the equimolar mixture, $\langle\cos\theta(r)\rangle$ for CS_2/benzene pairs is illustrated in Figure 5. Note that the other molar fractions considered here furnish a very similar distribution of $\langle\cos\theta(r)\rangle$. From Figure 5, it becomes evident that pairs between CS_2 and benzene molecules at shortest distances of 3.2 Å correspond to very small values of cos θ. Thus, first contact pairs of CS_2 and benzene exhibit preferentially a parallel configuration. However, as indicated by the very small amplitude in the $g(r)$ for the CS_2/benzene pairs from Figure 4, there are only a few closest-contact pairs, and one might assume that these short-range CS_2/benzene pairs with a parallel relative configuration correspond to the repulsive part of the intermolecular pair potential. At larger distance, $\langle\cos\theta\rangle$ increases rapidly presenting a broad maximum between 5 and 6 Å with an amplitude of 0.55 indicating a tendency to form more CS_2/benzene pairs in perpendicular configurations. This region of intermolecular distances corresponds to the peak maximum of the COM−COM pair distribution function for CS_2/benzene pairs in Figure 4. At long distances, Figure 5 presents the expected average value of $\langle\cos\theta\rangle = 0.5$ for CS_2 molecules randomly oriented relative to the benzene molecules.

More detailed orientational correlations between pairs of molecules can be obtained combining the pair distribution function $g(r)$ with the angular distribution for the angle θ,

$$g(r,\theta) = \frac{1}{N\rho}\left\langle\sum_{i=1}^{N}\sum_{j\neq i}^{N}\delta(r - r_{ij})\delta(\theta - \theta_{ij})\right\rangle \qquad (12)$$

In Figure 6, we present $g(r,\theta)$ for the CS_2/benzene pairs in the equimolar mixture. A broad short-range shoulder with angles

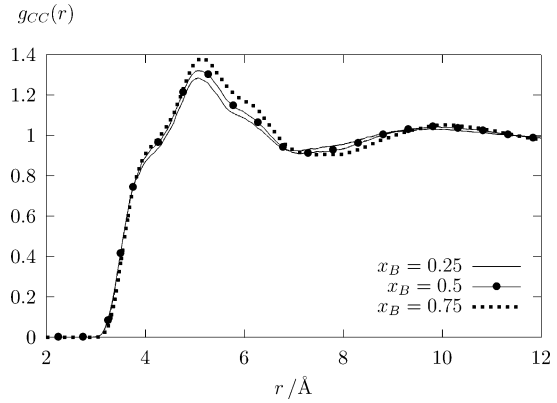

Figure 7. Carbon−carbon pair distribution function $g_{CC}(r)$ for CS_2−benzene pairs as a function of the molar fraction x_B for the benzene component.

TABLE 6: Atom−Atom Distances (Å) for the CS_2/Benzene Pair from ab Initio Calculations[7a]

b	C_A-C_B			C_B-S			COM_A-COM_B
a	5.66			4.18	7.17		5.49
b	4.38	4.79	5.19	4.66	5.38	6.05	4.60

[a] The subscript A denotes CS_2 and B the benzene molecule. [b] a represents CS_2 oriented along the C_6-axis of the benzene molecule. b represents CS_2 within the C_2-axis over bonds of the benzene molecule.

close to 90° indicates that pair configurations with the CS_2 molecules almost parallel to the benzene ring dominate up to distances of approximately 4.5 Å. CS_2 oriented perpendicular to the benzene ring system become important at distances between 5 and 6 Å corresponding to the peak position of the first maximum in the pair distribution function for the CS_2/benzene pairs shown in Figure 4. Beyond the first coordination shell, the orientational preferences disappear as illustrated by Figure 6.

In Figure 7, we depict the carbon−carbon pair distribution function, $g_{CC}(r)$, for CS_2/benzene pairs. For the CS_2 molecule, the COM coincides with the carbon atom, and in the benzene molecule, the carbon atom is only slightly dislocated from the COM. Consequently, the $g_{CC}(r)$ resembles many features of the corresponding COM−COM pair distribution function for CS_2/benzene pairs from Figure 4. However, both the short- and the long-range branch of the first maximum is more structured in the $g_{CC}(r)$ as a consequence of some preferential orientations. A parallel configuration with the CS_2 molecule within the C_2-axis over C−C bonds of the benzene molecule has been determined by ab initio calculations on the CS_2/benzene pair.[7] Some structural data obtained from these calculations are summarized in Table 6. The parallel configuration was characterized by a COM−COM distance of 4.6 Å, corresponding more or less to the short-distance shoulder with angles distributed around 90° from Figure 6. Three distinct distances between the carbon atoms of the benzene molecule and the carbon atoms of the CS_2 molecules at 4.38, 4.79, and 5.19 Å have been revealed by the ab initio calculations. These distances correspond perfectly to the short-range branch of the first maximum in the $g_{CC}(r)$ from Figure 7. The long-range branch in the $g_{CC}(r)$ is more affected by the perpendicular configuration between CS_2 and benzene. The ab initio calculations furnish a C−C distance of 5.66 Å for such a configuration, which corresponds to the region in the $g_{CC}(r)$ beyond the maximum.

In Figure 8, the pair distribution function of the benzene's carbon atoms and the S atoms is illustrated. A first maximum with distances of 4 Å can be coordinated to the perpendicular

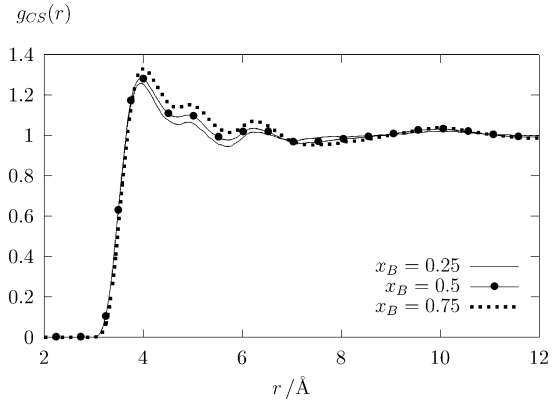

Figure 8. Carbon−sulfur pair distribution function $g_{CS}(r)$ for CS_2−benzene pairs as a function of the molar fraction x_B for the benzene component.

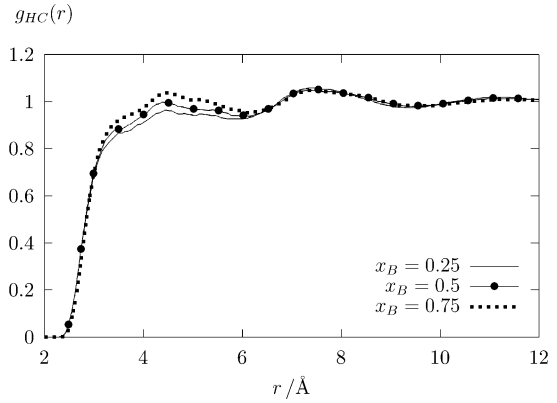

Figure 9. Hydrogen−carbon pair distribution function $g_{HC}(r)$ for CS_2−benzene pairs as a function of the molar fraction x_B for the benzene component.

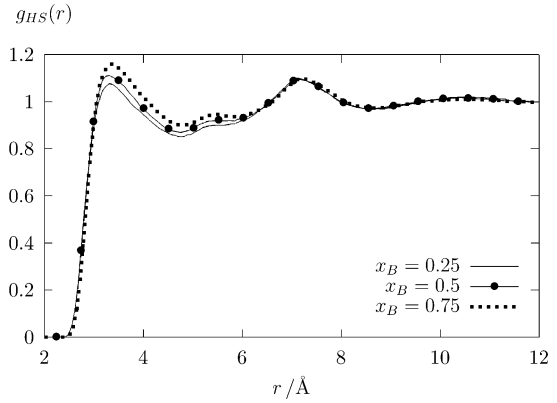

Figure 10. Hydrogen−sulfur pair distribution function $g_{HS}(r)$ for CS_2−benzene pairs as a function of the molar fraction x_B for the benzene component.

configuration between CS_2/benzene pairs. The corresponding ab initio distance from Table 6 is 4.18 Å. The structured features beyond the peak maximum in the $g_{CS}(r)$ are due to parallel configurations between CS_2 and benzene molecules. This configuration exhibits three distinct ab initio distances between the benzene's carbon atom and the S atom of the CS_2 molecule (Table 6) corresponding to the range beyond the peak maximum from Figure 8.

Finally, in Figures 9 and 10, we demonstrate the pair distributions for the benzene's hydrogen atoms and the CS_2's carbon ($g_{HC}(r)$, Figure 9) and sulfur atoms ($g_{HS}(r)$, Figure 10). The $g_{HC}(r)$ is only weakly structured and does not indicate any

characteristic peak positions. In contrast, the $g_{HS}(r)$ from Figure 10 presents a first peak at 3.5 Å that can be explained by the perpendicular configurations between benzene rings and CS_2 molecules similar to those in the $g_{CS}(r)$. A second maximum at distances slightly larger than 7 Å is expected for the second S atom in a perpendicularly oriented CS_2 molecule.

5. Conclusions

MD simulations have been employed to investigate thermodynamic properties and structural features of CS_2/C_6H_6 liquid mixtures at 298 K and benzene mole fractions of $x = 0.25$, 0.50, and 0.75. The potential models have been constructed by using well-known Lennard-Jones potentials of the pure compounds and describing the quadrupolar electrostatic interactions by point quadrupole moments located at the COMs of the molecules.

Calculated enthalpies of vaporization present a good agreement with experimental values for all of the compositions. From internal energies, we conclude that the binary liquid mixture of CS_2 and benzene is almost ideal. This conclusion is corroborated by the local mole fraction analysis clearly indicating that any changes in the first coordination shells around CS_2 or benzene can be explained by density effects.

Structural parameters obtained from angular and atom−atom pair distributions for CS_2/benzene pairs furnish preferentially perpendicular orientations between CS_2 and benzene molecules within the first coordination shell in agreement with experimental light scattering data.[6] However, first contact pairs of CS_2 and benzene molecules are oriented in parallel. Distances from ab initio calculations on the CS_2/benzene pair[7] confirm the relative orientations obtained from the liquid-state simulations.

The good agreement between the experimental results and the properties obtained from the simulations validates the employed potential model for the binary liquid system CS_2/benzene, at least for the accurate description of equilibrium properties. Currently, we are investigating whether this force field proposal is also able to correctly describe dynamical features of the mixtures as revealed by far-infrared absorption[4] and depolarized Rayleigh light scattering.[6]

References and Notes

(1) Francois, J.; Gan, J. Y. S.; Guenet, J. M. *Macromolecules* **1986**, *19*, 2755. Guenet, J. M.; Klein, M.; Menelle, A. *Macromolecules* **1989**, *22*, 493. Lehsaini, N.; Francois, J.; Well, G. *Macromolecules* **1993**, *26*, 7333.

(2) Chen, S. J.; Berry, G. C.; Plazek, D. J. *Macromolecules* **1995**, *28*, 6539.

(3) Morgan, R. S.; McAdon, J. M. *Int. J. Pept. Protein Res.* **1980**, *15*, 177. Nemethy, G.; Scheraga, H. A. *Biochem. Biophys. Res. Commun.* **1981**, *98*, 482. Reid, K. S. C.; Lindley, P. F.; Thornton, J. M. *FEBS Lett.* **1985**, *190*, 209. Kumar, M.; Lu, W. P.; Ragsdale, S. W. *Biochemistry* **1994**, *33*, 9769. Pranata, J. *Bioorg. Chem.* **1997**, *25*, 213. Zauhar, R. J.; Colbert, C. L.; Morgan, R. S.; Welsh, W. J. *Biopolymers* **2000**, *53*, 233.

(4) Zoidis, E.; Samios, J.; Dorfmüller, T. *Chem. Phys.* **1992**, 168, 349. Zoidis, E.; Dorfmüller, T. *Chem. Phys.* **1995**, *196*, 171.

(5) Zoidis, E. *Chem. Phys.* **1996**, *205*, 407.

(6) Zoidis, E.; Dorfmüller, T. *J. Mol. Liq.* **1995**, *64*, 263.

(7) Silveira, N. P.; Rodembusch, F. S.; Pereira, F. V.; Samios, D.; Livotto, P. R. *Chem. Phys.* **2000**, *253*, 165.

(8) Nandel, F. S.; Jain, D. V. S. *Indian J. Chem., Sect. A* **1984**, *23*, 543.

(9) Stassen, H. *J. Mol. Struct. (THEOCHEM)* **1999**, *464*, 107.

(10) Tildesley, D. J.; Madden, P. A. *Mol. Phys.* **1981**, *42*, 1137.

(11) Madden, P. A.; Tildesley, D. J. *Mol. Phys.* **1985**, *55*, 969. Geiger, L. C.; Ladanyi, B. M. *J. Chem. Phys.* **1987**, *87*, 191. Stassen, H.; Steele, W. A. *J. Chem. Phys.* **1995**, *103*, 4408.

(12) Samios, J.; Mittag, U.; Dorfmüller, T. *Mol. Phys.* **1986**, *59*, 65. Stassen, H.; Steele, W. A. *Mol. Phys.* **1996**, *89*, 1603.

(13) Stassen, H.; Steele, W. A. *Mol. Phys.* **1999**, *96*, 1269.

(14) Mittag, U.; Samios, J.; Dorfmüller, T. *Mol. Phys.* **1989**, *66*, 51.

(15) Mittag, U.; Samios, J.; Dorfmüller, T. *Mol. Phys.* **1994**, *81*, 1143.

(16) Stassen, H.; Dorfmüller, T. *Ber. Bunsen-Ges. Phys. Chem.* **1991**, *95*, 995. Stassen, H.; Samios, J.; Mittag, U. In *Molecular Liquids: New Perspective in Physics and Chemistry*; Teixeira-Dias, J. J. C., Ed.; NATO ASI Series C; Kluwer Academic Publishers: Dordrecht, The Netherlands, 1992; Vol. 379, p 549. Samios, J.; Mittag, U. *J. Phys. Chem.* **1994**, *98*, 2033.

(17) Williams, J. H.; Amos, R. D. *Chem. Phys. Lett.* **1979**, *66*, 370.

(18) Evans, D. J.; Watts, R. O. *Mol. Phys.* **1976**, *31*, 83. Steinhauser, O. *Chem. Phys.* **1982**, *73*, 155. Jorgensen, W. L.; Madura, J. D.; Swenson, C. J. *J. Am. Chem. Soc.* **1984**, *106*, 6638. Claessens, M.; Ferrario, M.; Ryckaert, J. P. *Mol. Phys.* **1983**, *50*, 217.

(19) Shi, X.; Bartell, L. S. *J. Phys. Chem.* **1988**, *92*, 5667. Bartell, L. S.; Sharkeyand, L. R.; Shi, X. *J. Am. Chem. Soc.* **1988**, *110*, 7006.

(20) Williams, D. E. *J. Chem. Phys.* **1967**, *47*, 4680.

(21) Cabaço, M. I.; Danten, Y.; Besnard, M.; Guissani, Y.; Guillot, B. *J. Phys. Chem. B* **1997**, *101*, 6977.

(22) Linse, P. *J. Am. Chem. Soc.* **1984**, *106*, 5425.

(23) Karlström, G.; Linse, P.; Wallqvist, A.; Jönsson, B. *J. Am. Chem. Soc.* **1983**, *105*, 3777.

(24) Jorgensen, W. L.; Severance, D. L. *J. Am. Chem. Soc.* **1990**, *112*, 4768.

(25) Allen, M. P.; Tildesley, D. J. *Computer Simulation of Liquids*; Clarendon Press: Oxford, U.K., 1987.

(26) Gray, C. G.; Gubbins, K. E. *Theory of Molecular Fluids, Vol. 1: Fundamentals*; Clarendon Press: Oxford, U.K., 1984.

(27) Experimental heats of vaporization have been computed from the pure liquid data using experimental excess enthalpies of mixing from Hill, R. J.; Swinton, F. L. *J. Chem. Thermodyn.* **1980**, *12*, 489.

(28) Gratias, R.; Kessler, H. *J. Phys. Chem. B* **1998**, *102*, 2027.

(29) Vaisman, I. I.; Berkowitz, M. L. *J. Am. Chem. Soc.* **1992**, *114*, 7889.

(30) Puhovski, Y. P.; Rode, B. M. *J. Phys. Chem.* **1995**, *99*, 1566.

(31) Nakanishi, K.; Toukubo, K. *J. Chem. Phys.* **1979**, *70*, 5848. Schoen, M.; Hoheisel, C. *Mol. Phys.* **1984**, *53*, 1367.

(32) Ebata, H.; Tokuda, J.; Maruyama, K.; Misawa, M. *J. Phys. Soc. Jpn.* **1998**, *67*, 2747.

(33) Danten, Y.; Guillot, B.; Guissani, Y. *J. Chem. Phys.* **1992**, *96*, 3782.

(34) Cabaço, M. I.; Danten, Y.; Besnard, M.; Guissani, Y.; Guillot, B. *J. Phys. Chem. B* **1998**, *102*, 10712.

(35) Chelli, R.; Cardini, G.; Procacci, P.; Righini, R.; Califano, S. *J. Chem. Phys.* **2000**, *113*, 6851.